Chinese Physical Society | IOP Publishing

CPB
Chinese Physics B

http://cpb.iphy.ac.cn https://iopscience.iop.org/journal/1674-1056

[Collective modes of Weyl fermions with repulsive S-wave interaction](#)

Xun-Gao Wang(王勋高), Huan-Yu Wang(王寰宇), Jiang-Min Zhang(张江敏), Wu-Ming Liu(刘伍明)

Citation: Chin. Phys. B . 2020, 29(11): 117201 . **doi:** 10.1088/1674-1056/abbbdb

Journal homepage: http://cpb.iphy.ac.cn; http://iopscience.iop.org/cpb

What follows is a list of articles you may be interested in

Generating two-dimensional quantum gases with high stability

Bo Xiao(肖波), Xuan-Kai Wang(王宣恺), Yong-Guang Zheng(郑永光), Yu-Meng Yang(杨雨萌), Wei-Yong Zhang(章维勇), Guo-Xian Su(苏国贤), Meng-Da Li(李梦达), Xiao Jiang(江晓), Zhen-Sheng Yuan(苑震生)

Chin. Phys. B . 2020, 29(7): 076701 . **doi:** 10.1088/1674-1056/ab8ac8

Accelerate Bose-Einstein condensate by interaction

Jie-Li Qin(秦杰利)

Chin. Phys. B . 2019, 28(12): 126701 . **doi:** 10.1088/1674-1056/ab4e8a

Propagation of dark soliton interacting with domain wall in two immiscible Bose-Einstein condensates

Lang Zheng(郑浪), Yi-Cai Zhang(张义财), Chao-Fei Liu(刘超飞)

Chin. Phys. B . 2019, 28(11): 116701 . **doi:** 10.1088/1674-1056/ab457e

Expansion dynamics of a spherical Bose-Einstein condensate

Rui-Zong Li(李睿宗), Tian-You Gao(高天佑), Dong-Fang Zhang(张东方), Shi-Guo Peng(彭世国), Ling-Ran Kong(孔令冉), Xing Shen(沈星), Kai-Jun Jiang(江开军)

Chin. Phys. B . 2019, 28(10): 106701 . **doi:** 10.1088/1674-1056/ab4177

Bloch oscillation of Weyl metal along synthetic dimensions

Ye Xiong(熊烨)

Chin. Phys. B . 2018, 27(12): 126701 . **doi:** 10.1088/1674-1056/27/12/126701

Chin. Phys. B Vol. 29, No. 11 (2020) 117201

RAPID COMMUNICATION

Collective modes of Weyl fermions with repulsive S-wave interaction*

Xun-Gao Wang(王勋高)[1,2], Huan-Yu Wang(王寰宇)[1,2], Jiang-Min Zhang(张江敏)[3,4], and Wu-Ming Liu(刘伍明)[1,2,5,†]

[1] *Beijing National Laboratory for Condensed Matter Physics, Institute of Physics, Chinese Academy of Sciences, Beijing* 100190, *China*
[2] *School of Physical Sciences, University of Chinese Academy of Sciences, Beijing* 100190, *China*
[3] *Fujian Provincial Key Laboratory of Quantum Manipulation New Energy Materials College of Physics and Energy, Fujian Normal University, Fuzhou* 350007, *China*
[4] *Fujian Provincial Collaborative Innovation Center for Optoelectronic Semiconductors and Efficient Devices, Xiamen* 361005, *China*
[5] *Songshan Lake Materials Laboratory, Dongguan* 523808, *China*

(Received 27 August 2020; revised manuscript received 11 September 2020; accepted manuscript online 28 September 2020)

We calculate the spin and density susceptibility of Weyl fermions with repulsive S-wave interaction in ultracold gases. Weyl fermions have a linear dispersion, which is qualitatively different from the parabolic dispersion of conventional materials. We find that there are different collective modes for the different strengths of repulsive interaction by solving the poles equations of the susceptibility in the random-phase approximation. In the long-wavelength limit, the sound velocity and the energy gaps vary with the different strengths of the interaction in the zero sound mode and the gapped modes, respectively. The particle–hole continuum is obtained as well, where the imaginary part of the susceptibility is nonzero.

Keywords: ultracold gases, collective modes, random-phase approximation

PACS: 72.15.nj, 67.85.–d **DOI:** 10.1088/1674-1056/abbbdb

1. Introduction

The Dirac materials have attracted a great deal of attention since the discovery of graphene. For example, high-temperature d-wave superconductors, topological insulator, Dirac semi-metals, and Weyl semi-metals have been researched recently.[1–5] These materials possess an identical property of linear dispersion in the low-energy excitations near the Dirac or Weyl nodes.

Recently, the experimental realizations of the Weyl semimetals have led to wide study on collective behavior of Weyl semimetals in condensed matter physics,[6–10] and some experimental schemes have been proposed in ultracold atomic gases to obtain the Weyl fermions.[11,12] However, there is little investigation for collective behavior of Weyl fermions in ultracold atomic gases. Motivated by these experimental schemes, we investigate the collective properties near the single Weyl node model with repulsive S-wave interaction. It is an interesting problem in many-particle systems to study some novel collective modes.[13–17] In contrast to the Coulomb interaction among electrons in metals or semi-conductors, the S-wave interaction among ultracold atoms can be modulated by the technique of Feshbach resonance.[18,19] The low-energy S-wave interaction in ultracold atomic gases is determined by the scattering length a_{s}. The collective modes are obtained by solving the poles equation of the spin and density susceptibility within the random-phase approximation (RPA).[20–25]

Our paper is organized as follow. In Section 2 we present the model for the three-dimensional Fermi gas with repulsive S-wave interaction. Here, the eigenvalues and eigenstates of the model Hamiltonian are obtained, and all the parameters are explained. We proceed to calculate the bare spin and density susceptibility in terms of the Green's functions and solve collective modes via the poles of the susceptibility in the random-phase approximation. The dispersion relations for the modes are shown by numerically solving the RPA equation in Section 3. Finally, we give the summation over our paper.

2. The model and calculation

We consider a low-energy effective model for a single Weyl point with repulsive S-wave interaction in the three-dimensional fermionic system. The effective Hamiltonian is of the form ($\hbar$ is taken as 1 in our paper)

$$\begin{aligned}\mathcal{H} =& \sum_{\boldsymbol{k},\alpha,\beta} c^{\dagger}_{\boldsymbol{k},\alpha}\left(v_{\mathrm{F}}\boldsymbol{k}\cdot\boldsymbol{\sigma}_{\alpha\beta}-\mu\delta_{\alpha,\beta}\right)c_{\boldsymbol{k},\beta}\\ &+2g\sum_{\boldsymbol{k},\boldsymbol{k}',\boldsymbol{q}} c^{\dagger}_{\boldsymbol{k}+\boldsymbol{q},\uparrow}c^{\dagger}_{\boldsymbol{k}'-\boldsymbol{q},\downarrow}c_{\boldsymbol{k}',\downarrow}c_{\boldsymbol{k},\uparrow},\end{aligned}\tag{1}$$

where v_{F} is the Fermi velocity and $\mu = v_{\mathrm{F}}k_{\mathrm{F}}$ is the chemical potential where we consider only the Fermi surface is above the Weyl node, namely, $\mu = v_{\mathrm{F}}k_{\mathrm{F}}$ larger than zero, and k_{F} is the Fermi momentum. α and β are the spin (pseudo-spin) indexes. The first term is the noninteracting term of Hamiltonian, whose eigenstates can be obtained as

$$|\boldsymbol{k},+\rangle = \begin{pmatrix}\cos\frac{\theta}{2}\\ \sin\frac{\theta}{2}\,\mathrm{e}^{\mathrm{i}\phi}\end{pmatrix},\quad |\boldsymbol{k},-\rangle = \begin{pmatrix}\sin\frac{\theta}{2}\\ -\cos\frac{\theta}{2}\,\mathrm{e}^{\mathrm{i}\phi}\end{pmatrix},\tag{2}$$

*Project supported by the National Natural Science Foundation of China (Grant No. 2016YFA0301500).
†Corresponding author. E-mail: wliu@iphy.ac.cn
 http://iopscience.iop.org/cpb http://cpb.iphy.ac.cn

where θ and ϕ are the polar angle and the azimuth angle in wave vector space, respectively. The helicity $\pm$ represents the spin polarization. The eigenvalues of energy corresponding to the eigenstates are $\xi_{k,\pm} = \pm v_{\mathrm{F}} k - \mu$. We note that the spin and the momentum are intimately locked. The locking effect shows that the spin and the momentum are in the same direction in the upper branch band and are in the opposite directions in the lower branch band. The second term in Eq. (1) represents the S-wave interaction in ultracold atomic gases. The low-energy interaction among ultracold atoms is generally determined by the scattering length a_{s}, which can be modulated by Feshbach resonances experimentally. The significance of S-wave interaction in ultracold atoms could be characterized by the dimensionless ratio of the average interaction and kinetic energy $\varepsilon_{\mathrm{int}}/\varepsilon_{\mathrm{kin}}$.

In what follows, we choose the spin and density susceptibility as the investigating response function, which can be written as

$$\chi^{\mu\nu}(q,\mathrm{i}\omega_m) = \sum_{k,p}\sum_{\alpha\beta\gamma\delta}\int_0^\beta \mathrm{d}\tau\, \mathrm{e}^{\mathrm{i}\omega_m\tau} \times \left\langle T_\tau c^\dagger_{k,\alpha}\sigma^\mu_{\alpha\beta}c_{k+q,\beta}(\tau)c^\dagger_{p+q,\gamma}\sigma^\nu_{\gamma\delta}c_{p,\delta}(0)\right\rangle, \quad (3)$$

where μ, ν have four indexes, and $\sigma^\mu, \sigma^\nu = (1, \sigma_z, \sigma^+, \sigma^-)$. $\sigma^\pm = \sigma_x \pm \mathrm{i}\sigma_y$ represent the raising and lowing operators. α, β, γ, and δ denote the spin up or down. In Matsubara formalism, we can express the bare spin and density susceptibility $\chi_{\mathrm{b}}^{\mu\nu}$ in terms of the noninteracting Green's function

$$\chi_{\mathrm{b}}^{\mu\nu}(\boldsymbol{q},\mathrm{i}q_m) = -k_{\mathrm{B}}T\sum_{\boldsymbol{k},\mathrm{i}k_n}\mathrm{Tr}\big[G^0(\boldsymbol{k}+\boldsymbol{q}/2,ik_n)\sigma^\mu \times G^0(\boldsymbol{k}-\boldsymbol{q}/2,\mathrm{i}k_n-\mathrm{i}q_m)\sigma^\nu\big], \quad (4)$$

and the noninteracting Green's function is given by

$$G^0_{\alpha\beta}(\boldsymbol{k},\mathrm{i}k_n) = \sum_{s=\pm1}\frac{(P_s)_{\alpha\beta}}{\mathrm{i}k_n - \xi_{\boldsymbol{k},s}}, \quad (5)$$

where P_s is the projection operator with respect to the helicity eigenstates.

In order to calculate the susceptibilities, it is convenient to introduce an overlap factor, which has the form

$$F^{\mu\nu}_{sr} = \mathrm{Tr}\left[P_s(\boldsymbol{k}+\boldsymbol{q}/2)\sigma^\mu P_r(\boldsymbol{k}-\boldsymbol{q}/2)\sigma^\nu\right], \quad (6)$$

where s, r denote the helicity indexes. After some reductions and taking the analytical continuation $\mathrm{i}q_m \to \omega + \mathrm{i}0^+$, the susceptibility can be written as

$$\chi_{\mathrm{b}}^{\mu\nu}(q,\omega) = -\sum_{k,s,r}F^{\mu\nu}_{sr}\frac{n_{\mathrm{F}}(\xi_{k-q/2,r}) - n_{\mathrm{F}}(\xi_{k+q/2,s})}{\xi_{k-q/2,r} - \xi_{k+q/2,s} + \omega + \mathrm{i}0^+}, \quad (7)$$

where $n_{\mathrm{F}}(\xi)$ is the Fermi distribution function. At zero temperature, the distribution function is just the Heaviside step function $n_{\mathrm{F}}(\xi) = \Theta(-\xi)$. The overlap factor contains two contributions from intrasubband and intersubband. In the long-wavelength limit $|\boldsymbol{q}| \to 0$, the overlap factor $F^{\mu\nu}$ can be expanded with respect to $\boldsymbol{q}$ and retain only up to the first order of q. The intrasubband contribution is

$$F_{s,s} = \begin{pmatrix} 1 & s\cos(\theta) & A_{13}\,\mathrm{e}^{\mathrm{i}\phi} & A_{14}\,\mathrm{e}^{-\mathrm{i}\phi} \\ s\cos(\theta) & (\cos\theta)^2 & A_{23}\,\mathrm{e}^{\mathrm{i}\phi} & A_{24}\,\mathrm{e}^{-\mathrm{i}\phi} \\ A_{31}\,\mathrm{e}^{\mathrm{i}\phi} & A_{32}\,\mathrm{e}^{\mathrm{i}\phi} & A_{33}\,\mathrm{e}^{2\mathrm{i}\phi} & \left(1+s\dfrac{|q|}{|2k|}\right)(\sin\theta)^2 \\ A_{41}\,\mathrm{e}^{-\mathrm{i}\phi} & A_{42}\,\mathrm{e}^{-\mathrm{i}\phi} & \left(1-s\dfrac{|q|}{|2k|}\right)(\sin\theta)^2 & A_{44}\,\mathrm{e}^{-2\mathrm{i}\phi} \end{pmatrix}. \quad (8)$$

The intersubband contribution is

$$F_{s,-s} = \begin{pmatrix} 0 & s\dfrac{|q|}{2\,|k|}(\sin\theta)^2 & B_{13}\,\mathrm{e}^{\mathrm{i}\phi} & B_{14}\,\mathrm{e}^{-\mathrm{i}\phi} \\ s\dfrac{|q|}{2\,|k|}(\sin\theta)^2 & (\sin\theta)^2 & B_{23}\,\mathrm{e}^{\mathrm{i}\phi} & B_{24}\,\mathrm{e}^{-\mathrm{i}\phi} \\ B_{31}\,\mathrm{e}^{\mathrm{i}\phi} & B_{32}\,\mathrm{e}^{\mathrm{i}\phi} & B_{33}\,\mathrm{e}^{2\mathrm{i}\phi} & (1+s\cos\theta)^2 \\ B_{41}\,\mathrm{e}^{-\mathrm{i}\phi} & B_{42}\,\mathrm{e}^{-\mathrm{i}\phi} & (1-s\cos\theta)^2 & B_{44}\,\mathrm{e}^{-2\mathrm{i}\phi} \end{pmatrix}. \quad (9)$$

In the long-wavelength limit ($q \ll k_{\mathrm{F}}$), the expansions of the distribution function and the particle–hole excitations energy with respect to q up to the first order for the intrasubband and intersubband are given by

$$n_{\mathrm{F}}(\xi_{k+q/2,+}) - n_{\mathrm{F}}(\xi_{k-q/2,+}) \simeq -\delta(|\boldsymbol{k}| - k_{\mathrm{F}})\hat{k}\cdot q, \quad (10)$$

$$n_{\mathrm{F}}(\xi_{k+q/2,s}) - n_{\mathrm{F}}(\xi_{k-q/2,-s}) \simeq s(\Theta(-\xi_{k,+}) - 1) - \delta(\xi_{k,+})v_{\mathrm{F}}\hat{k}\cdot q/2, \quad (11)$$

with

$$\xi_{k+q/2,s} - \xi_{k-q/2,s} \simeq s v_{\mathrm{F}}\hat{k}\cdot q, \quad (12)$$

$$\xi_{k+q/2,s} - \xi_{k-q/2,-s} \simeq s v_{\mathrm{F}}\,|k|\,. \quad (13)$$

By substituting these expressions into Eq. (7) and performing an elementary integral over k, we can obtain the intrasubband and intersubband susceptibilities respectively, which can be written as

$$\chi_{\text{intra}} = \alpha \begin{pmatrix} f & yf & 0 & 0 \\ yf & \frac{2}{3}+y^2 f & 0 & 0 \\ 0 & 0 & 0 & f-(\frac{2}{3}+y^2 f) \\ 0 & 0 & f-(\frac{2}{3}+y^2 f) & 0 \end{pmatrix}, \quad (14)$$

$$\chi_{\text{inter}} = \alpha \begin{pmatrix} 0 & 0 & 0 & 0 \\ 0 & \frac{2}{3}F & 0 & 0 \\ 0 & 0 & 0 & \frac{4}{3}F \\ 0 & 0 & \frac{4}{3}F & 0 \end{pmatrix}, \quad (15)$$

where $\alpha = \frac{Vk_{\text{F}}^3}{(2\pi)^2 v_{\text{F}} k_{\text{F}}}$, $y = \frac{\omega}{v_{\text{F}} q}$, $f = 2 + y \ln\left|\frac{y-1}{y+1}\right|$, and $F = \bar{\Lambda}^2 - 1 + \frac{\bar{\omega}^2}{2} \ln\left|\frac{4\bar{\Lambda}^2-\bar{\omega}^2}{4-\bar{\omega}^2}\right|$, and we set $\frac{Vk_{\text{F}}^3}{v_{\text{F}} k_{\text{F}}} = 1$ for calculation in our paper. Λ denotes an ultraviolet cut-off of momentum for the wave vector integrals to conveniently deal with the infinite Fermi sea in the lower branch band, and the dimensionless parameters $\bar{\Lambda} = \Lambda / k_{\text{F}}$, $\bar{\omega} = \omega / (v_{\text{F}} k_{\text{F}})$. Here, we just only retain the real part of the integral because the image part of the spin and density susceptibility existing corresponds to particle–hole continuum regions, which are shown in Fig. 1. The purple region illustrates that the particles occupied the lower branch band are excited to the upper branch band, and the yellow region represents the excitations only in the upper branch band.

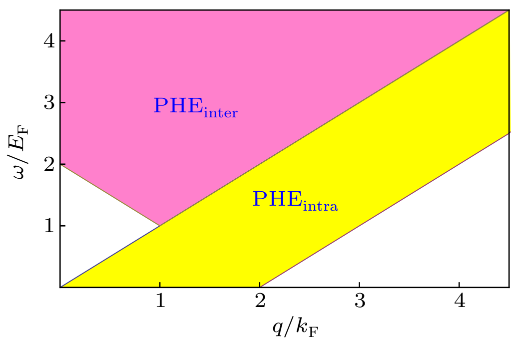

Fig. 1. Particle–hole continuum (Landau damping regime) in Weyl fermions. The purple region and the yellow region represent intersubband particle–hole excitations (PHE$_{\text{inter}}$) and intrasubband particle–hole excitations (PHE$_{\text{intra}}$), respectively.

In the random phase approximation, we can conclude the relationship between the RPA susceptibility and the bare susceptibility

$$\chi_{\text{RPA}}^{\mu\nu}(q, \text{i}\omega_m) = \chi_{\text{b}}^{\mu\rho}(q, \text{i}\omega_m) \left(\frac{1}{1 + g\eta\chi_{\text{b}}(q, \text{i}q_m)} \right)^{\rho\nu}, \quad (16)$$

where $\eta = \text{diag}(1, -1, -1, -1)$.

3. Theoretical and numerical results

In order to find the collective modes, we need to obtain the solutions of the poles equation of the spin and density susceptibility. From the above results, the bare susceptibility can be grouped into two 2×2 submatrices. One matrix describes the coupling between density and longitudinal spin, and the other describes the coupling between two transverse spins. First, we investigate the collective modes in the long-wavelength limit by calculating the poles equation of the RPA susceptibility. Then we can obtain the dispersion relationship beyond the long-wavelength limit by using a numerical calculation.

It is reasonable to assume that q is oriented along with the z direction. In the long-wavelength limit, the density and longitudinal spin correction function is given by

$$\chi_{nS_z} = \alpha \begin{pmatrix} f & yf \\ yf & \frac{2}{3}+y^2 f + \frac{2}{3}F \end{pmatrix}. \quad (17)$$

We assume that the the dimensionless parameter y is a finite value for $\omega \to 0$ and an infinite when ω is a finite value. Substituting Eq. (17) into Eq. (16), we obtain the poles equation

$$(1 + g\alpha f)\left(1 - g\alpha\left[\frac{2}{3} + y^2 f + \frac{2}{3}F\right]\right) + (g\alpha y f)^2 = 0. \quad (18)$$

Solving this poles equation, one result can be obtained when ω tends to zero, so we can show y varied with the interaction strength g, which is plotted in Fig. 2. Apparently, y is the sound velocity of zero sound, which represents a gapless mode. The other result can be obtained when ω is a finite value, which corresponds to the gapped modes. The gap associated with the interaction strength is illustrated in Fig. 3.

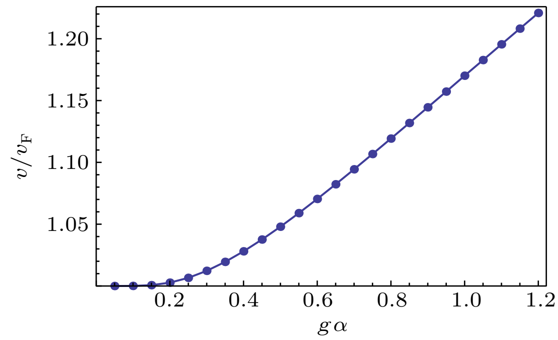

Fig. 2. A sketch of the interaction strength dependence of the sound velocity in the long-wave length limit for the zero sound mode. Here we use the cut-off momentum $\bar{\Lambda} = 10$.

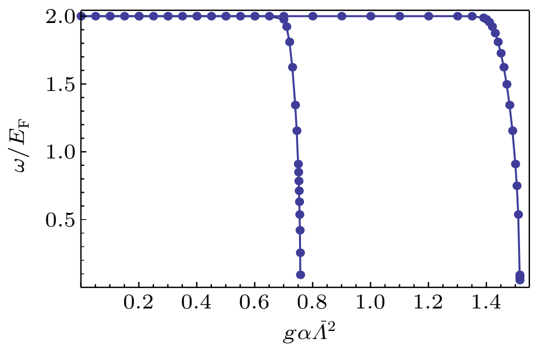

Fig. 3. A sketch of the interaction strength dependence of the gap in the long-wave length limit for the gapped modes. There are two branches of gapped modes when $g\alpha\bar{\Lambda}^2 < 0.7575$, which corresponds to the dimensionless interaction strength $g < 0.299$, but there is only one branch of gapped mode when $0.7575 < g\alpha\bar{\Lambda}^2 < 1.515$, Here we use $\bar{\Lambda} = 10$.

In a similar way, the transverse spin correction function is given by

$$\chi_{S^+S^-} = \alpha \begin{pmatrix} 0 & \frac{4}{3}F + f - \left(\frac{2}{3} + y^2 f\right) \\ \text{h.c.} & 0 \end{pmatrix}. \tag{19}$$

The corresponding poles equation can be obtained as

$$1 - g^2\alpha^2 \left(\frac{4}{3}F + f - \left(\frac{2}{3} + y^2 f\right)\right)^2 = 0. \tag{20}$$

The two branches of gapped modes can be found by solving the poles equation when $g \simeq 0.299$, and there is one branch of gapped mode when $0.7575 < g\alpha\bar{\Lambda}^2 < 1.515$. The gapped solutions are shown in Fig. 3.

Finally, we calculate the dispersion relations beyond the long-wavelength limit by using a numerical method. The different modes can exist with the different repulsive interaction strengths. We calculate the dispersion relations in the chosen g of 10, 0.46, 0.218, which are illustrated in Figs. 4–6, respectively. In fact, the three typical interaction strengthes represent different phase domains. In the long-wavelength limit, we can obtain one gapless solution which corresponds to the zero sound mode when g is larger than around 0.598, one gapped solution when g is between 0.299 and 0.598, and two gapped solutions when g is smaller than ∼0.299. We cannot draw the second gapped dispersion, but we are sure of the existence of the gapped solution according to the continuity of the poles with respect to ω.

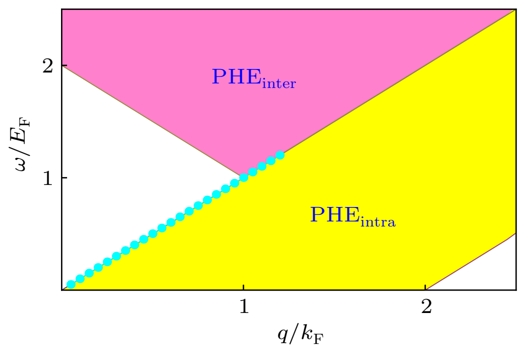

Fig. 4. Dispersion of the collective modes for the zero sound mode. The dispersion is close to the boundary of the intrasubband particle–hole excitations continuum region from above. Here we use $g = 10, \bar{\Lambda} = 10$.

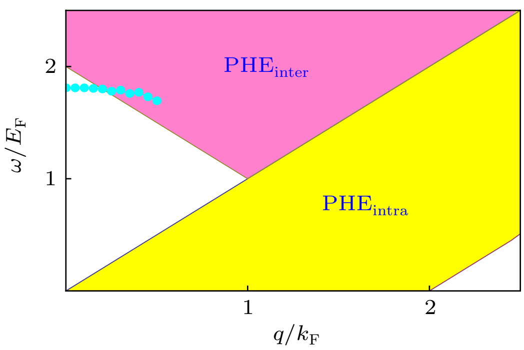

Fig. 5. Dispersion of the collective modes for the one branch of gapped mode. Here we use $g = 0.46, \bar{\Lambda} = 10$.

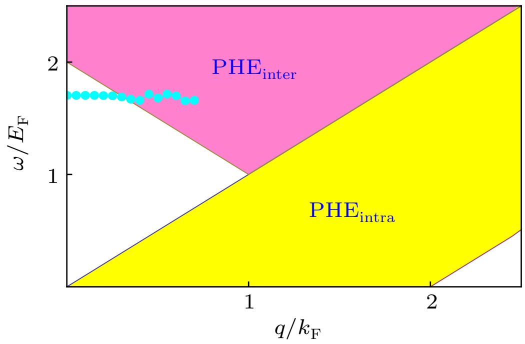

Fig. 6. Dispersion of the collective modes for the one branch of mode. The other branch of gapped mode is very close to the boundary of the intersubband particle–hole excitations continuum region. Here we use $g = 0.218, \bar{\Lambda} = 10$.

4. Conclusion

We evaluate the collective modes in a three-dimensional fermion system governed by Weyl Hamiltonian with repulsive S-wave interaction. It is clear that the system has the linear particle–hole excitations. In the long-wavelength limit, we find that there is the zero sound mode when g is larger than 0.598, one gapped mode when g is between 0.299 and 0.598, and there are two gapped modes when g is smaller than 0.299 for the momentum cut-off $\bar{\Lambda} = 10$. In contrast to the fixed Coulomb interaction in condensed matter, we can find the relationships between the sound velocity or the gap and the interaction strength, which can be tuned into a large range of values by Feshbach resonance in ultracold atoms. The dispersion relations of collective modes are obtained in three given interaction strengthes.

Acknowledgment

We are grateful to Zhang ShangShun for constructive discussions.

References

[1] Yang B J and Nagaosa N 2014 *Nat. Commun.* **5** 4898
[2] Potter A C, Kimchi I and Vishwanath A 2014 *Nat. Commun.* **5** 5161
[3] Rosenstein B, Shapiro B Y, Li D P and Shapiro I 2015 *J. Phys.: Condens. Matter* **27** 025701
[4] Kung H H, Maiti S, Wang X, Cheong S W, Maslov D L and Blumberg G 2017 *Phys. Rev. Lett.* **119** 136802
[5] Hasan M Z and Kane C L 2010 *Rev. Mod. Phys.* **82** 3045
[6] Wan X G, Turner A M, Vishwanath A and Savrasov S Y 2011 *Phys. Rev. B* **83** 205101
[7] Weng H M, Fang C, Fang Z, Bernevig B A and Dai X 2015 *Phys. Rev. X* **5** 011029
[8] Lv B Q, Weng H M, Fu B B, Wang X P, Miao H, Ma J, Richard P, Huang X C, Zhao L X, Chen G F, Fang Z, Dai X, Qian T and Ding H 2015 *Phys. Rev. X* **5** 031013
[9] Xu S Y, Belopolski I, Alidoust N, *et al.* 2015 *Science* **349** 613
[10] Lu L, Wang Z Y, Ye D X, Ran L X, Fu L, Joannopoulos J D and Soljacic M 2015 *Science* **349** 622
[11] Dubcek T, Kennedy C, Lu L, Ketterle W, Soljacic M and Buljan H 2015 *Phys. Rev. Lett.* **114** 225301
[12] He W Y, Zhang S Z and Law K T 2016 *Phys. Rev. A* **94** 013606

[13] Raghu S, Chung S B, Qi X L and Zhang S C 2010 *Phys. Rev. Lett.* **104** 116401
[14] Sachdeva R, Thakur A, Vignale G and Agarwal 2015 *Phys. Rev. B* **91** 205426
[15] Srivatsa N S and Ganesh R 2018 *Phys. Rev. B* **98** 165133
[16] Gorbar E V, Miransky V A, Shovkovy I A and Sukhachov P O 2019 *Phys. Rev. B* **99** 155120
[17] Lv M and Zhang S C 2013 *Int. J. Mod. Phys. B* **25** 1350177
[18] Kohler T, Goral K and Julienne P S 2006 *Rev. Mod. Phys.* **78** 1311
[19] Chin C, Grimm R, Julienne P and Tiesinga E 2010 *Rev. Mod. Phys.* **82** 1225
[20] Zhang S S, Yu X L, Ye J W and Liu W M 2013 *Phys. Rev. A* **87** 063623
[21] Ryan J C 1991 *Phys. Rev. B* **43** 4499
[22] Maiti S, Zyuzin V and Maslov D L 2015 *Phys. Rev. B* **91** 035106
[23] Kumar A and Maslov D L 2017 *Phys. Rev. B* **95** 165140
[24] Mir M and Abedinpour S H 2017 *Phys. Rev. B* **96** 245110
[25] Principi A, Polini M and Vignale G 2009 *Phys. Rev. B* **80** 075418